# Complex dynamics analysis of impulsively coupled Duffing oscillators with ring structure*

Jiang Hai-Bo(姜海波)[a)†], Zhang Li-Ping(张丽萍)[a)], and Yu Jian-Jiang(于建江)[b)]

[a)] School of Mathematics, Yancheng Teachers University, Yancheng 224002, China
[b)] School of Information Science and Technology, Yancheng Teachers University, Yancheng 224002, China

(Received 18 June 2014; revised manuscript received 10 September 2014; published online 10 December 2014)

Impulsively coupled systems are high-dimensional non-smooth systems that can exhibit rich and complex dynamics. This paper studies the complex dynamics of a non-smooth system which is unidirectionally impulsively coupled by three Duffing oscillators in a ring structure. By constructing a proper Poincaré map of the non-smooth system, an analytical expression of the Jacobian matrix of Poincaré map is given. Two-parameter Hopf bifurcation sets are obtained by combining the shooting method and the Runge–Kutta method. When the period is fixed and the coupling strength changes, the system undergoes stable, periodic, quasi-periodic, and hyper-chaotic solutions, etc. Floquet theory is used to study the stability of the periodic solutions of the system and their bifurcations.

**Keywords:** impulsively coupled oscillators, bifurcation, periodic solutions, Floquet theory

**PACS:** 05.45.Ac, 05.45.Pq **DOI:** 10.1088/1674-1056/24/2/020502

## 1. Introduction

Coupled oscillators have been intensively studied in various disciplines because they have a variety of applications, including pattern recognition, biological information processing, and control.[1–7] Very recently, the dynamics of special networks of coupled oscillators has received particular attention in the literature.[8–11] In Ref. [8], the authors investigated different dynamical states of synchronization in a ring of four mutually inertia coupled self-sustained electrical systems, which are described by coupled Rayleigh–Duffing equations, and presented the stability properties of periodic solutions and transition boundaries between different dynamical states using the Floquet theory. In Refs. [9] and [10], the dynamic behaviors and synchronization of a ring of mutually coupled van der Pol oscillators were studied. The dynamics of a ring of unidirectionally coupled autonomous Duffing oscillators was studied in Ref. [11]. Although the individual uncoupled system has only one globally stable equilibrium, the system transits into periodic, quasi-periodic, and chaotic behaviors with an increase in coupling strength.

In practice there are many oscillators which do not interact with each other continuously, such as the species-food model in biology, the information transfer and exchange in ants, and the model of an integrated circuit. Very recently, impulsively coupled oscillators that are assumed to interact with each other only at discrete times have drawn considerable attention.[12–16] Pulse coupled neural networks which are special impulsively coupled oscillators have been utilized for various image processing applications, including image segmentation, feature generation, face extraction, motion detection, and so on.[12,13] In Ref. [14], a kind of impulsively coupled complex dynamical systems was introduced and several criteria related to the eigenvalues and eigenvectors of coupling matrix for synchronizing the impulsively coupled complex dynamical systems were established. In Ref. [15], a class of impulsively coupled complex switched networks with parametric uncertainties and time-varying delays was introduced and the robust synchronization of the presented model was studied. In Ref. [16], the authors introduced the concept of partial contraction theory of impulsive systems and investigated the synchronization problem of impulsively coupled oscillators. On the other hand, networked dynamical systems can achieve synchronization without interacting with each other continuously.[17–20] In Refs. [17]–[19], a kind of impulsive control protocol has been introduced for networked linear and nonlinear dynamical systems, respectively.

On the other hand, the dynamics of a system with an impulsive effect has attracted increasing attention.[21–31] In Ref. [21], the authors investigated the bifurcation and chaos observed in coupled Bonhoeffer–van der Pol (BVP) neurons with external impulsive forces. A class of periodic motions of an inverted pendulum forced by impulsive periodic excitation was analyzed in Ref. [22]. In Ref. [23], the authors investigated the effect of periodic forcing and impulsive perturbations on the predator–prey model with Holling type-II functional response. The onset of nontrivial periodic solutions

*Project supported by the National Natural Science Foundation of China (Grant Nos. 11402224, 11202180, 61273106, and 11171290), the Qing Lan Project of the Jiangsu Higher Educational Institutions of China, and the Jiangsu Overseas Research and Training Program for University Prominent Young and Middle-aged Teachers and Presidents.

†Corresponding author. E-mail: yctcjhb@gmail.com

© 2015 Chinese Physical Society and IOP Publishing Ltd 

for an integrated pest management model which is subject to pulsed biological and chemical controls was investigated in Ref. [24]. In Refs. [25]–[27], the dynamical behaviors of a linear impulsive system and a prey–predator system with impulsive control were discussed, respectively. In Ref. [28], the complex dynamics of the Chen system via an impulsive force was investigated and the Floquet theory was used to explore the non-smooth bifurcation mechanism for the periodic solutions. Furthermore, Floquet theory has been extended to explore the bifurcation mechanism for the periodic solutions of the Logistic map via periodic impulsive forces in Refs. [29] and [30].

In this paper, the complex dynamics of the non-smooth system which is unidirectionally impulsively coupled by three Duffing oscillators in a ring structure is studied both theoretically and numerically. The main contributions of this paper include: 1) the analytical expression of the Jacobian matrix of Poincaré map is derived by constructing a proper Poincaré map; 2) the two-parameter Hopf bifurcation sets are given by combining the shooting method and the Runge–Kutta method; and, 3) complex behaviors of the system are explored when the period is fixed and the coupling strength changes, and the stability of the periodic solutions of the system and their bifurcations are studied by using the Floquet theory.

The remainder of this paper is organized as follows. In Section 2, the system model is formulated. In Section 3, a bifurcation analysis of impulsively coupled Duffing oscillators is presented. In Section 4, bifurcation and chaos in impulsively coupled Duffing oscillators are explored when the impulsive coupling period is fixed and the impulsive coupling strength is considered as a bifurcation parameter. Finally, our conclusions are drawn in Section 5.

**Notation** Throughout this paper, the superscripts '$-1$' and 'T' stand for the inverse and transpose of a matrix, respectively; $\mathbb{R}^n$ denotes the $n$-dimensional Euclidean space; Let $\mathbb{R}_+ = [0,\infty)$, $\mathbb{N} = \{0,1,2,\ldots\}$, $\mathbb{Z}_+ = \{1,2,\ldots\}$; $\mathbb{R}^{n\times m}$ is the set of all $n\times m$ real matrices; For a vector $x \in \mathbb{R}^n$, let $||x||$ denote the Euclidean vector norm, i.e., $||x|| = \sqrt{x^{\mathrm{T}}x}$; j is the imaginary unit with the property $\mathrm{j}^2 = -1$.

## 2. System model

Consider the autonomous Duffing oscillator described by the following second-order ordinary differential equation (ODE):

$$\ddot{v} + d\dot{v} + av + v^3 = 0, \tag{1}$$

where $a$ and $d$ are positive constants. In this paper, the fixed parameters $a = 0.1$, $d = 0.3$ are used. Introducing the new coordinates $x = v$, $y = \dot{v}$ to Eq. (1), the dynamics of the Duffing oscillator can be described as

$$\begin{aligned} \dot{x} &= y, \\ \dot{y} &= -dy - ax - x^3, \end{aligned} \tag{2}$$

The system (2) only has one single stable equilibrium point at $(x,y) = (0,0)$, which is shown in Fig. 1.

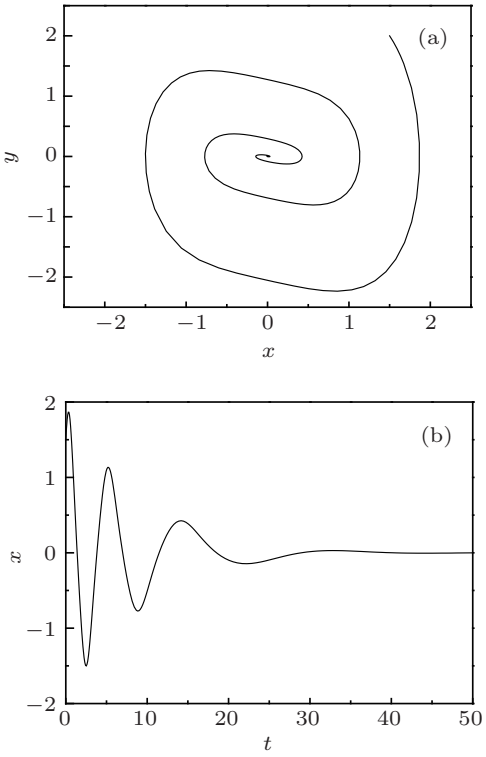



**Fig. 1.** Phase portrait and time histories of system (2) at $a = 0.1$ and $d = 0.3$.

Consider the ring of unidirectionally impulsively coupled Duffing oscillators, as shown in Fig. 2. The dynamics of impulsively coupled Duffing oscillators can be described by the following system

$$\begin{cases} \dot{x}^i = y^i, \\ \dot{y}^i = -dy^i - ax^i - (x^i)^3, \end{cases} \quad t \neq k\tau, k \in \mathbb{N},$$
$$\begin{cases} \Delta x^i = x^i(t^+) - x^i(t^-) = 0, \\ \Delta y^i = y^i(t^+) - y^i(t^-) = h(x^{i-1} - x^i), \end{cases} \quad t = k\tau, k \in \mathbb{N}, \tag{3}$$

where $\tau$ is the impulsive coupling period, $h$ is the impulsive coupling strength,

$$x^i(t^+) = \lim_{\gamma\to 0^+} x^i(t+\gamma), \quad x^i(t^-) = \lim_{\gamma\to 0^-} x^i(t+\gamma),$$

$i = 1,2,3$. Assume that $x^i(t^+) = x^i(t)$, $y^i(t^+) = y^i(t)$, that is the solution $(x^1(t), y^1(t), x^2(t), y^2(t), x^3(t), y^3(t))$ of the system is right-continuous at $k\tau$.

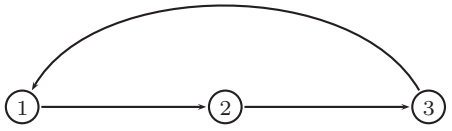



**Fig. 2.** Schematic representation of the ring network.

## 3. Bifurcation analysis

Since impulsively coupled systems are high-dimensional non-smooth systems, bifurcation analysis methods for continuous systems are not available. Therefore, the bifurcation analysis methods for non-smooth systems proposed in Refs. [21], [24], [32], and [33] are adopted in this paper to explore the bifurcation phenomenon of impulsively coupled Duffing oscillators.

The solution of Eq. (3) is described as

$$\begin{aligned} x^i(t) &= \varphi^i(t-t_0,x_0^1,y_0^1,x_0^2,y_0^2,x_0^3,y_0^3,h,\tau),\\ y^i(t) &= \phi^i(t-t_0,x_0^1,y_0^1,x_0^2,y_0^2,x_0^3,y_0^3,h,\tau), \end{aligned} \tag{4}$$

and

$$\begin{aligned} \varphi^i(t_0,x_0^1,y_0^1,x_0^2,y_0^2,x_0^3,y_0^3,h,\tau) &= x_0^i,\\ \phi^i(t_0,x_0^1,y_0^1,x_0^2,y_0^2,x_0^3,y_0^3,h,\tau) &= y_0^i, \end{aligned}$$

where $(x_0^1,y_0^1,x_0^2,y_0^2,x_0^3,y_0^3)$ is the initial value and $i=1,2,3$.

Define the map $P_1$ as

$$\begin{aligned} P_1 : {} & (x^1,y^1,x^2,y^2,x^3,y^3)\to\\ & (x^1,y^1+h(x^3-x^1),x^2,y^2+h(x^1-x^2),\\ & x^3,y^3+h(x^2-x^3)), \end{aligned}$$

and define the map $P_2$ as

$$\begin{aligned} P_2 : {} & (x^1,y^1,x^2,y^2,x^3,y^3)\to\\ & (\varphi^1(\tau,x^1,y^1,x^2,y^2,x^3,y^3,h,\tau),\\ & \phi^1(\tau,x^1,y^1,x^2,y^2,x^3,y^3,h,\tau),\\ & \varphi^2(\tau,x^1,y^1,x^2,y^2,x^3,y^3,h,\tau),\\ & \phi^2(\tau,x^1,y^1,x^2,y^2,x^3,y^3,h,\tau),\\ & \varphi^3(\tau,x^1,y^1,x^2,y^2,x^3,y^3,h,\tau),\\ & \phi^3(\tau,x^1,y^1,x^2,y^2,x^3,y^3,h,\tau)). \end{aligned}$$

Then, the Poincaré map $P$ can be defined as $P=P_2\circ P_1$, which is a composition of $P_1$ and $P_2$.

Let a fixed point of the Poincaré map $P$ be $u(x^1,y^1,x^2,y^2,x^3,y^3)$ and the fixed point satisfies

$$u=P(u). \tag{5}$$

If the Poincaré map $P$ has a fixed point, then the system has a periodic solution with period $\tau$ which is called a $1T$-periodic solution. Similarly, if the Poincaré map $P$ has a $k$-periodic point $u(x^1,y^1,x^2,y^2,x^3,y^3)$, i.e., $u=P^k(u)$ and $u\neq P^m(u)$, $m=1,2,\ldots,k-1$, then the system has a periodic solution with period $k\tau$, which is called a $kT$-periodic solution.

The characteristic equation of the fixed point $u$ of the Poincaré map $P$ is

$$\det(\mu I-DP(u))=0, \tag{6}$$

where $DP(u)$ is the Jacobian matrix of the Poincaré map $P$ at $u$.

The conditions for the bifurcations of the fixed point are given as follows:[21]

(i) When $\mu=1$, the system generates tangent bifurcation (also known as saddle-node bifurcation),

(ii) When $\mu=-1$, the system generates period-doubling bifurcation, and

(iii) When $\mu=\mathrm{e}^{\mathrm{j}\theta}$, $0<\theta<\pi$, the system generates Hopf bifurcation (also known as Neimark–Sacker bifurcation).

The Jacobian matrix of the Poincaré map $P_1$ is

$$DP_1=\begin{pmatrix} 1 & 0 & 0 & 0 & 0 & 0\\ -h & 1 & 0 & 0 & h & 0\\ 0 & 0 & 1 & 0 & 0 & 0\\ h & 0 & -h & 1 & 0 & 0\\ 0 & 0 & 0 & 0 & 1 & 0\\ 0 & 0 & h & 0 & -h & 1 \end{pmatrix}.$$

The numerical solution of the Jacobian matrix $DP_2$ of the Poincaré map $P_2$ can be determined by combining the shooting method and the Runge–Kutta method. Since $P=P_2\circ P_1$, it follows that the analytical expression of the Jacobian matrix of Poincaré map is $DP=DP_2\times DP_1$. Now the impulsive coupling period and impulsive coupling strength are considered as bifurcation parameters, so that the bifurcation set and eigenvalues of the Jacobian matrix $DP$, i.e., the Floquet multipliers $\mu_1,\mu_2,\mu_3,\mu_4,\mu_5,\mu_6$ are obtained by solving Eqs. (5) and (6). Let $h\in(0,5]$, the Hopf bifurcation curve for the system is then obtained as depicted in Fig. 3. From Fig. 3, there exists a relation between the impulsive coupling period, impulsive coupling strength, and Hopf bifurcation. When the impulsive coupling period is larger, the impulsive coupling strength needs to be larger so that the system can generate a Hopf bifurcation. On the other hand, when the impulsive coupling period is smaller, the impulsive coupling strength needs to be smaller so that the system can generate a Hopf bifurcation.

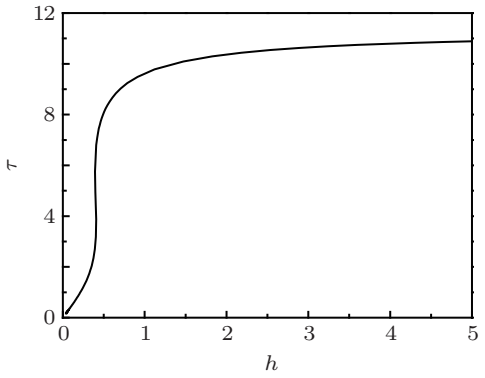



**Fig. 3.** Hopf bifurcation curve for system (3) at $a=0.1$ and $d=0.3$.

## 4. Bifurcation and chaos

In this section, the impulsive coupling period is fixed at $\tau=2$ and the impulsive coupling strength $h$ is considered as a bifurcation parameter. The effect of the parameter $h$ on the system is considered by the stroboscopic map. The main idea is stated as follows: for a fixed $h$ over a range, the numerical solution is first obtained; then, the stroboscopically sampling state of the system, i.e., the state of the system after periodic

impulsive forcing, with period $\tau$ is obtained. Thus, the bifurcation diagram describing the effect of the impulsive forces can be attained. The stroboscopic map is a special case of the Poincaré map for periodically forced system or periodically pulsed system. Fixed points of the stroboscopic map correspond to $1T$-periodic solutions of the system (3) whose period is $\tau$; periodic points of period $k$ of the stroboscopic map correspond to $kT$-periodic solutions of the system (3) whose period is $k\tau$; invariant circles correspond to quasi-periodic solutions of the system (3).[23]

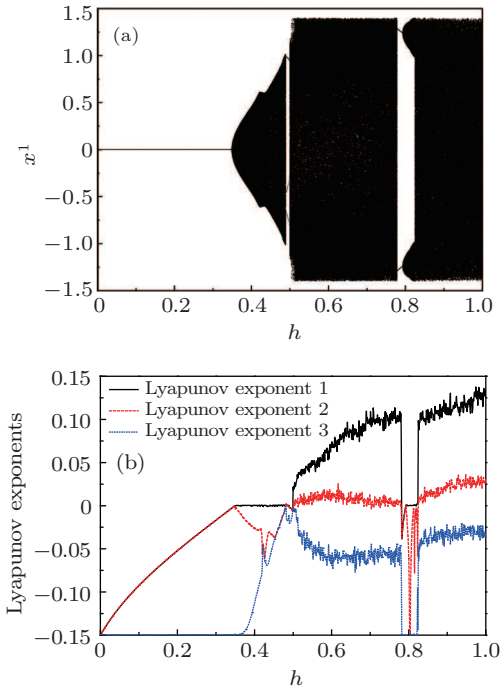



**Fig. 4.** (color online) Bifurcation and Laypunov exponents diagrams for system (3) under varying coupling strength $h$ at $a = 0.1$ and $d = 0.3$.

The bifurcation and the Laypunov exponents diagrams of the system (3) are shown in Fig. 4. Here the Laypunov exponents of the system (3) are calculated by using the Poincaré map and the Gram–Schmidt orthonormalization method.[32] From Fig. 4, when $h > 0$, as $h$ increases, the system transits into stable, quasi-periodic, periodic, and hyper-chaotic solutions, etc. In the following, the dynamical behaviors will be analyzed by using the Floquet theory.

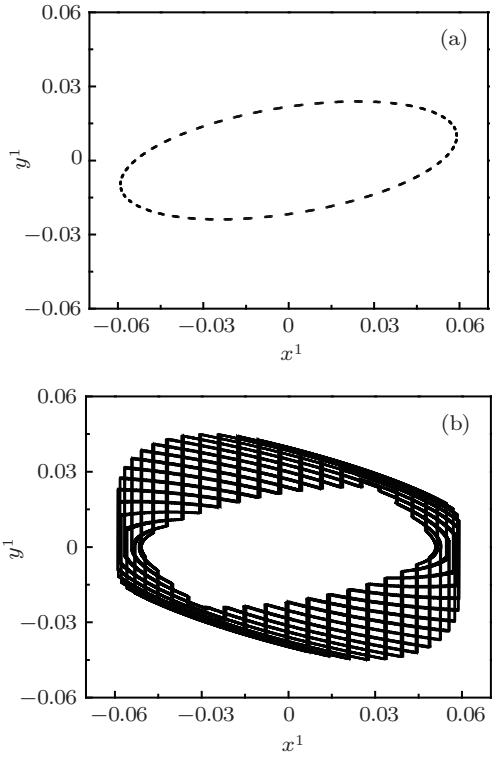



**Fig. 5.** Quasi-periodic solution for system (3) at $a = 0.1$, $d = 0.3$, and $h = 0.35$. (a) Stroboscopic map; (b) phase portrait.

As can be seen from Fig. 4, when $h < 0.349$, the system shows a stable equilibrium solution and all of the Floquet multipliers lie inside the unit circle. At $h = 0.349$, a pair of two complex conjugate Floquet multipliers crosses the unit circle and the other Floquet multipliers stay inside the unit circle, so the Hopf bifurcation occurs and the equilibrium solution falls into a quasi-periodic solution, as shown in Fig. 5. This result is consistent with Figs. 3 and 4. Near $h = 0.349$, the Floquet characteristic multipliers are shown in Table 1.

**Table 1.** Floquet characteristic multipliers for system (3) at $a = 0.1$ and $d = 0.3$ (near $h = 0.349$).

| $h$ | $\mu_{1,2}$ | $\lvert\mu_{1,2}\rvert$ | $\mu_{3,4}$ | $\lvert\mu_{3,4}\rvert$ | $\mu_{5,6}$ | $\lvert\mu_{5,6}\rvert$ |
|---|---|---|---|---|---|---|
| 0.309 | 0.3838 ± 0.8945i | 0.9733 | 0.6289 ± 0.3915i | 0.7408 | 0.2223 ± 0.5182i | 0.5638 |
| 0.319 | 0.3722 ± 0.9065i | 0.9800 | 0.6289 ± 0.3915i | 0.7408 | 0.2127 ± 0.5180i | 0.5600 |
| 0.329 | 0.3606 ± 0.9184i | 0.9867 | 0.6289 ± 0.3915i | 0.7408 | 0.2033 ± 0.5177i | 0.5562 |
| 0.339 | 0.3488 ± 0.9301i | 0.9934 | 0.6289 ± 0.3915i | 0.7408 | 0.1940 ± 0.5173i | 0.5525 |
| 0.349 | 0.3369 ± 0.9417i | 1.0001 | 0.6289 ± 0.3915i | 0.7408 | 0.1848 ± 0.5167i | 0.5487 |

In Fig. 6, invariant circles are observed in the stroboscopic maps of the quasi-periodic solutions and these invariant circles gradually become large with their shape changing from smooth to non-smooth as $h$ increases from 0.355 to 0.481. At $h = 0.49888$, the invariant circle loses its stability and the state moves to a stable $3T$-periodic solution, as depicted in Fig. 7. Near $h = 0.49888$, a pair of two complex conjugate Floquet multipliers passes through the unit circle, one real Floquet multiplier jumps outside the unit circle and the other Floquet multiplier stays inside the unit circle. Hence, the $3T$-periodic solution jumps to a chaotic solution instantly, which is shown in Fig. 8. Near $h = 0.49888$, the Floquet characteristic multipliers are shown in Table 2. At

$h = 0.5$, the Laypunov exponents of the system are 0.02177, 0.00253, −0.00629, −0.04207, −0.43896, and −0.43951. Since there are two positive Laypunov exponents, the system is hyper-chaotic at $h = 0.5$.

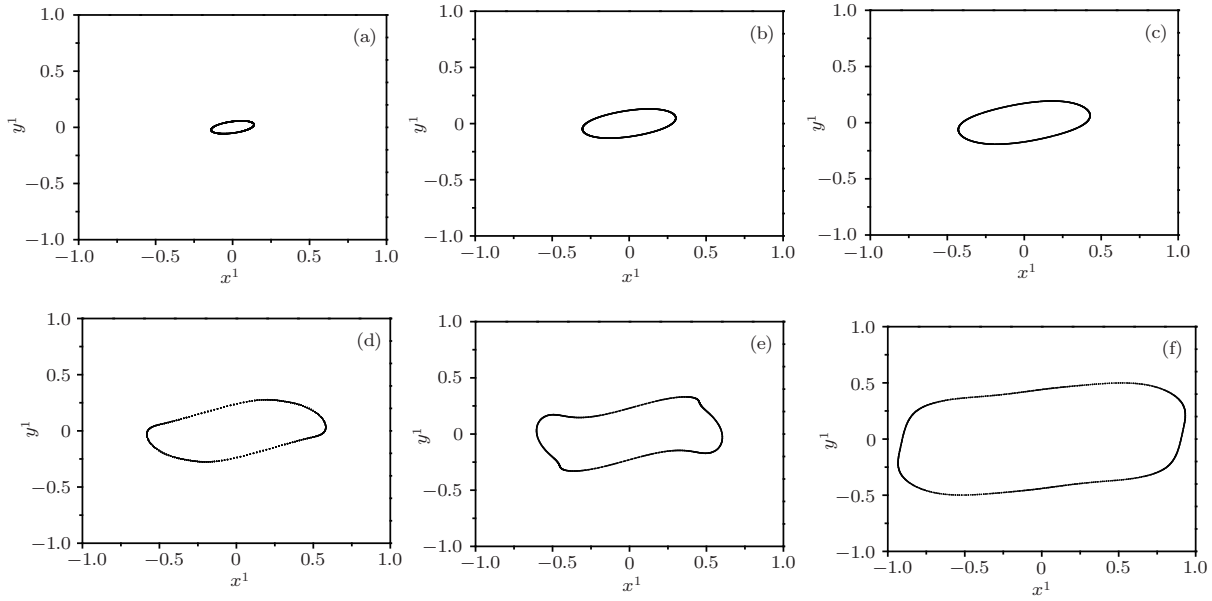



**Fig. 6.** Stroboscopic maps of quasi-periodic solutions for system (3) at $a = 0.1$ and $d = 0.3$. (a) $h = 0.355$; (b) $h = 0.375$; (c) $h = 0.395$; (d) $h = 0.417$; (e) $h = 0.43$; (f) $h = 0.481$.

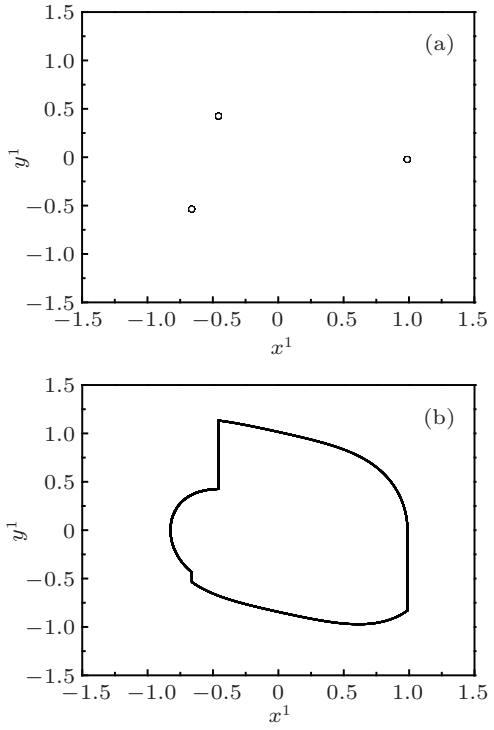



**Fig. 7.** $3T$-periodic solution for system (3) at $a = 0.1$, $d = 0.3$, and $h = 0.49$. (a) Stroboscopic map; (b) phase portrait.

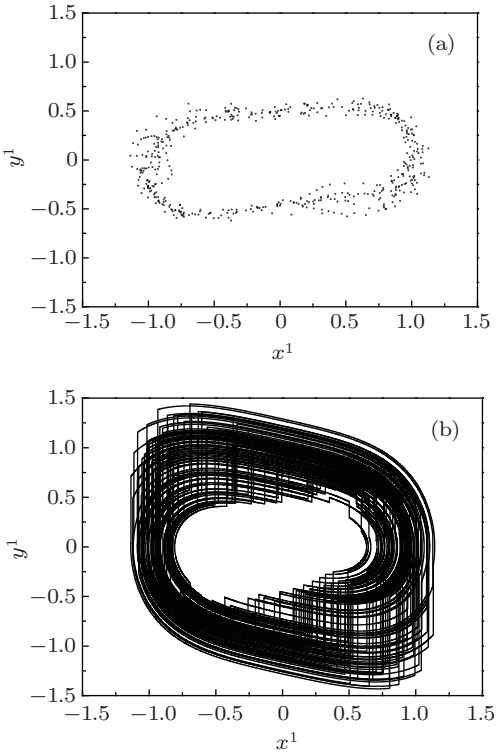



**Fig. 8.** Hyper-chaotic attractor for system (3) at $a = 0.1$, $d = 0.3$, and $h = 0.5$. (a) Stroboscopic map; (b) phase portrait.

**Table 2.** Floquet characteristic multipliers for system (3) at $a = 0.1$ and $d = 0.3$ (near $h = 0.49888$).

| $h$ | $\mu_{1,2}$ | $\lvert\mu_{1,2}\rvert$ | $\mu_{3,4}$ | $\lvert\mu_{3,4}\rvert$ | $\mu_{5,6}$ | $\lvert\mu_{5,6}\rvert$ |
|---|---|---|---|---|---|---|
| 0.49000 | 0.7403 ± 0.6531i | 0.9872 | 0.8721 ± 0.1479i | 0.8846 | 0.0465 ± 0.0612i | 0.0768 |
| 0.49500 | 0.7967 ± 0.5733i | 0.9815 | 0.8895 ± 0.1829i | 0.9081 | 0.0471 ± 0.0587i | 0.0753 |
| 0.49700 | 0.8403 ± 0.4908i | 0.9731 | 0.9076 ± 0.2086i | 0.9313 | 0.0476 ± 0.0567i | 0.0740 |
| 0.49800 | 0.8745 ± 0.4089i | 0.9654 | 0.9234 ± 0.2285i | 0.9513 | 0.0480 ± 0.0551i | 0.0731 |
| 0.49887 | 0.9421 ± 0.1076i | 0.9483 | 0.9585 ± 0.2669i | 0.9950 | 0.0485 ± 0.0521i | 0.0711 |
| 0.49888 | 1.2836, 0.6829 | 1.2836, 0.6829 | 0.9837 ± 0.2897i | 1.0255 | 0.0486 ± 0.0502i | 0.0699 |

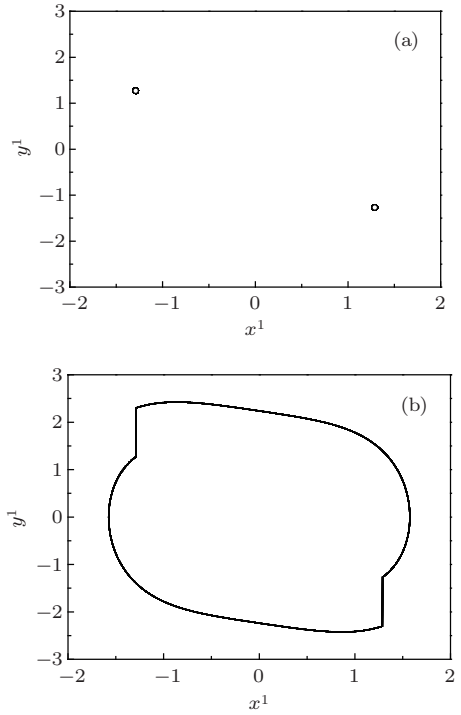



**Fig. 9.** $2T$-periodic solution for system (3) at $a = 0.1$, $d = 0.3$, and $h = 0.779$. (a) Stroboscopic map; (b) phase portrait.

The hyper-chaotic attractor lasts until $h = 0.779$. At $h = 0.779$, there is a boundary crisis and the hyper-chaotic attractor suddenly jumps to a stable $2T$-periodic solution, as depicted in Fig. 9. Thereafter, at $h = 0.790$, a pair of two complex conjugate Floquet multipliers crosses the unit circle and the other Floquet multipliers stay inside the unit circle. So another Hopf bifurcation occurs and the $2T$-periodic solution becomes a quasi-periodic solution, which brings out two closed invariant circles, as shown in Fig. 10. Near $h = 0.790$, the Floquet characteristic multipliers are shown in Table 3. With the increase of the impulsive coupling strength, these two invariant circles become four invariant circles, eight invariant circles, and so on, which can be called a torus doubling bifurcation cascade.[34] Finally, this torus doubling bifurcation cascade leads the quasi-periodic solutions to a chaotic solution, which is depicted in Figs. 11 and 12. At $h = 0.825$, the Laypunov exponents of the system are 0.09876, 0.00855, −0.04798, −0.20611, −0.34228, and −0.41643. Since there are two positive Lyapunov exponents, the system is hyper-chaotic at $h = 0.825$.

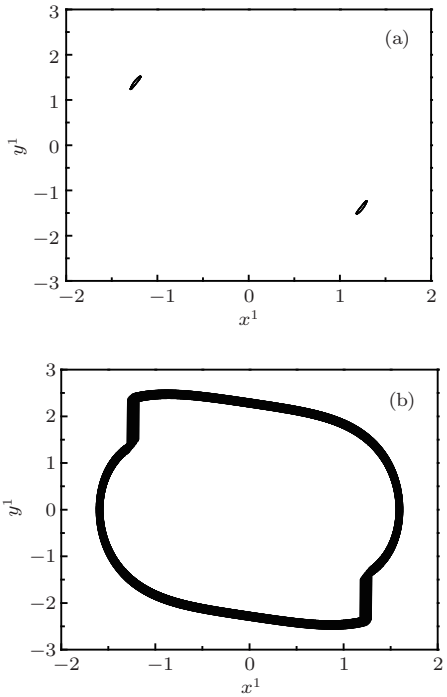



**Fig. 10.** Quasi-periodic solution for system (3) at $a = 0.1$, $d = 0.3$, and $h = 0.795$. (a) Stroboscopic map; (b) phase portrait.

**Table 3.** Floquet characteristic multipliers for system (3) at $a = 0.1$ and $d = 0.3$ (near $h = 0.790$).

| $h$ | $\mu_{1,2}$ | $\lvert\mu_{1,2}\rvert$ | $\mu_{3,4}$ | $\lvert\mu_{3,4}\rvert$ | $\mu_{5,6}$ | $\lvert\mu_{5,6}\rvert$ |
|---|---|---|---|---|---|---|
| 0.780 | 0.3199 ± 0.8232i | 0.8832 | –0.5177 ± 0.1820i | 0.5487 | 0.1232 ± 0.3172i | 0.3402 |
| 0.784 | 0.2965 ± 0.8963i | 0.9440 | –0.5172 ± 0.1834i | 0.5487 | 0.1000 ± 0.3022i | 0.3183 |
| 0.789 | 0.2669 ± 0.9622i | 0.9986 | –0.5167 ± 0.1847i | 0.5487 | 0.0804 ± 0.2900i | 0.3010 |
| 0.790 | 0.2613 ± 0.9735i | 1.0080 | –0.5167 ± 0.1848i | 0.5487 | 0.0773 ± 0.2880i | 0.2982 |

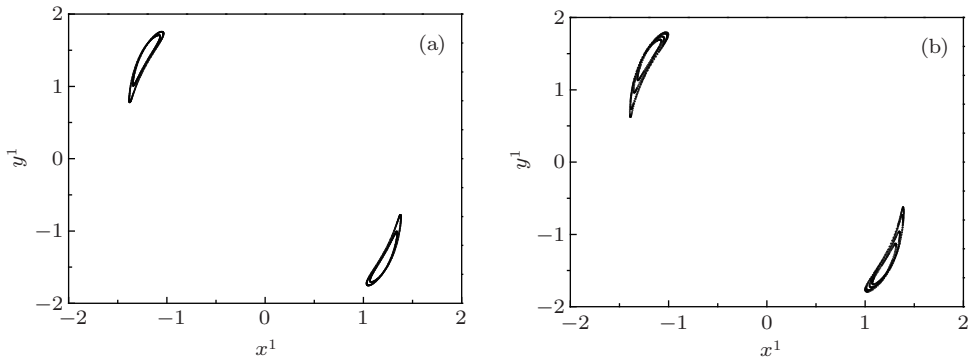



**Fig. 11.** Stroboscopic maps for system (3) at $a = 0.1$ and $d = 0.3$. (a) $h = 0.815$; (b) $h = 0.82$.

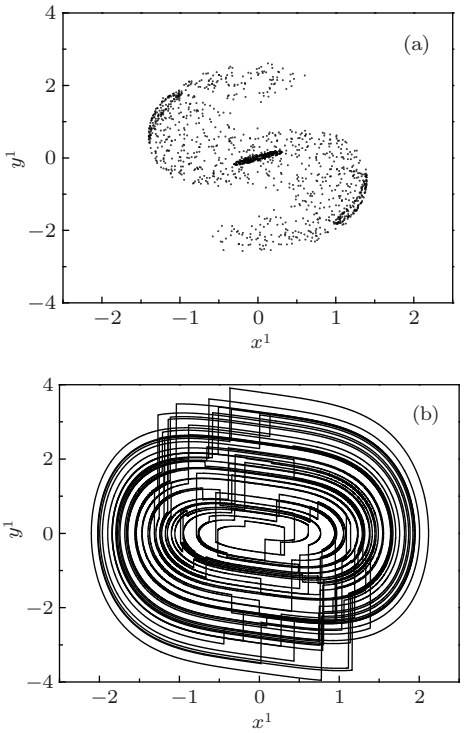



**Fig. 12.** Hyper-chaotic attractor for system (3) at $a = 0.1$, $d = 0.3$ and $h = 0.825$. (a) Stroboscopic map; (b) phase portrait.

This section only focuses on the dynamical behaviors of the system with the fixed period $\tau = 2$. However, we can also obtain similar complex dynamical behaviors of the system with other periods and the proposed method can also be used to explore the bifurcation mechanism of these complex dynamical behaviors.

## 5. Conclusions

This paper has studied the complex dynamics of a non-smooth system which is unidirectionally impulsively coupled by three Duffing oscillators in a ring structure. The analytical expression of the Jacobian matrix of the Poincaré map has been derived by constructing a proper Poincaré map and the two-parameter Hopf bifurcation sets have been given by combining the shooting method and the Runge–Kutta method. In particular, the impulsive coupling period is fixed at $\tau = 2$ and the impulsive coupling strength is considered as a control parameter. When the impulsive coupling strength $h \in (0, 0.349)$, the system has a stable equilibrium solution. At $h = 0.349$, the Hopf bifurcation of the stable equilibrium solution occurs and the system becomes a quasi-periodic solution. With a further increase of impulsive coupling strength from 0.349 to 0.490, the invariant circles change their shape and smoothness. At $h = 0.490$, the system suddenly jumps to a $3T$-periodic solution and then to a hyper-chaotic solution thereafter. The hyper-chaotic solution lasts until $h = 0.779$, where it jumps to a $2T$-periodic solution through a boundary crisis. Later on, the $2T$-periodic solution becomes a quasi-periodic solution via a Hopf bifurcation at $h = 0.790$. This is followed by a torus doubling bifurcation cascade, which eventually leads to a hyper-chaotic solution. Numerical observations have shown that impulsively coupled oscillators can exhibit rich and complex dynamics. This research can improve the understanding and practical application of impulsively coupled nonlinear systems. Our future work will investigate the complex dynamics of large networks of impulsively coupled oscillators.

## Acknowledgments

The authors are grateful to the anonymous reviewers for their valuable comments and suggestions, which have helped to improve the presentation of the paper. We also thank Prof. Bi Qin-Sheng, Dr. Zhang Chun and Dr. Liu Yang for their helpful comments.

## References

[1] Kuramoto Y 1984 *Chemical Oscillations, Wave, and Turbulence* (Berlin: Springer)
[2] Bi Q S 2007 *Phys. Lett. A* **369** 418
[3] Pikovsky A, Rosenblum M and Kurths J 2001 *Synchronization: A Universal Concept in Nonlinear Science* (Cambridge: Cambridge University Press)
[4] Strogatz S H 2000 *Physica D* **143** 1
[5] Fotsin H B and Woafo P 2005 *Chaos, Solitons and Fractals* **24** 1363
[6] Zhou J, Cheng X H, Xiang L and Zhang Y C 2007 *Chaos, Solitons and Fractals* **33** 607
[7] Wang Q Y and Lu Q S 2010 *Int. J. Non-Linear Mech.* **45** 640
[8] Rene Y 2006 *Physica A* **366** 187
[9] Barrón M A and Sen M 2009 *Nonlinear Dyn.* **56** 357
[10] Barron M A, Sen M and Corona E 2008 *Innovations and Advanced Techniques in Systems, Computing Sciences and Software Engineering* (Berlin: Springer Netherlands) 346
[11] Perlikowski P, Yanchuk S, Wolfrum M, Stefanski A, Mosiolek P and Kapitaniak T 2010 *Chaos* **20** 013111
[12] Mirollo R M and Strogatz S H 1990 *SIAM J. Appl. Math.* **50** 1645
[13] Nakano H and Saito T 2004 *IEEE Trans. Neural Networks* **15** 1018
[14] Han X P, Lu J A and Wu X Q 2008 *Int. J. Bifur. Chaos* **18** 1539
[15] Yang M, Wang Y W, Xiao J W and Wang H O 2010 *Nonlinear Anal. Real World Appl.* **11** 3008
[16] Jiang H B and Bi Q S 2012 *Nonlinear Dyn.* **67** 781
[17] Jiang H B, Yu J J and Zhou C G 2011 *Int. J. Systems Sci.* **42** 967
[18] Jiang H B and Bi Q S 2010 *Phys. Lett. A* **374** 2723
[19] Jiang H B, Bi Q S and Zheng S 2012 *Commun. Nonlinear Sci. Numer. Simul.* **17** 378
[20] Zhou J, Wu Q J and Xiang L 2012 *Nonlinear Dyn.* **69** 1393
[21] Kitajima H and Kawakami H 2001 *IEEE International Symposium on Circuit and Systems (ISCAS2001)*, May 6–9, 2001, Sydney, NSW, Vol. 2, p. 285
[22] Lenci S and Rega G 2000 *Chaos, Solitona and Fractals* **11** 2453
[23] Zhang S W, Tan D J and Chen L S 2006 *Chaos, Solitons and Fractals* **29** 474
[24] Georgescu P, Zhang H and Chen L S 2008 *Appl. Math. Comput.* **202** 675
[25] Jiang G R and Yang Q G 2008 *Chin. Phys. B* **17** 4114
[26] Jiang G R, Xu B G and Yang Q G 2009 *Chin. Phys. B* **18** 5235
[27] Qian L N, Lu Q S, Meng Q G and Feng Z S 2010 *J. Math. Anal. Appl.* **363** 345
[28] Jiang H B, Zhang L P, Chen Z Y and Bi Q S 2012 *Acta Phys. Sin.* **61** 080505 (in Chinese)
[29] Jiang H B, Li T, Zeng X L and Zhang L P 2013 *Acta Phys. Sin.* **62** 120508 (in Chinese)
[30] Jiang H B, Li T, Zeng X L and Zhang L P 2014 *Chin. Phys. B* **23** 010501
[31] Liu F, Guan Z H and Wang H O 2010 *Nonlinear Anal. Real World Appl.* **11** 1491
[32] Jin L, Lu Q S and Twizell E H 2006 *J. Sound Vibration* **298** 1019
[33] Dankowicz H and Schilder F 2011 *J. Comput. Nonlinear Dyn.* **6** 031003
[34] Zhang Y X and Luo G W 2013 *J. Sound Vibration* **332** 5462